River Flow 2010 - Dittrich, Koll, Aberle & Geisenhainer (eds) - © 2010 Bundesanstalt für Wasserbau ISBN 978-3-939230-00-7

Intercomparison of three morphodynamic models for the Lower Yellow River

J.Q. Xia[1,3], Z.B. Wang[2], B. van Maren[2], J.J. Zhou[3], B.S. Wu[3]

1 *State Key Laboratory of Water Resources and Hydropower Engineering Science, Wuhan University, Wuhan 430072, China*
2 *Faculty of Civil Engineering and Geosciences, Delft University of Technology, 2600 GA Delft, the Netherlands*
3 *State Key Laboratory of Hydroscience and Engineering, Tsinghua University, Beijing 100084, China*

ABSTRACT: Significant channel adjustment often occurs in the Lower Yellow River (LYR), and it is a challenging work to simulate the morphodynamic processes in the LYR using numerical models. An intercomparison of three morphodynamic models (Delft3D, 2DLLCDM and 2DRPM) for the LYR is presented herein. The models are first compared with each other in the model concepts, and are then used to simulate the morphodynamic processes in a braided reach of the LYR. The model predictions indicate that: (i) the hydrodynamic processes computed by all the three models agree well with the field data if an appropriate value of the roughness coefficient is used; (ii) the concentrations of suspended load at the downstream boundary computed by Delft3D and 2DLLCDM agree closely with the observed data, but there is a great difference between the concentrations calculated by 2DPRM and those measured; and (iii) the predicted changes of cross-sectional profiles do not correspond well with the measurements for all the models. Based on these findings, three urgent improvements are recommended for increasing the prediction accuracy in these models, including: the development of bed roughness predictor, the introduction of graded sediment transport capacity formulation, and the consideration of bank erosion module.

Keywords: Morphodynamic model, bed roughness, sediment transport capacity, morphological changes, Lower Yellow River

1 INTRODUCTION

The Yellow River (see Figure1), as the second largest river in China, is well known for its high concentrations of suspended load. Generally, the Lower Yellow River (LYR) is defined as the reach between Mengjin in Henan and Lijin in Shandong, with a total length of about 786 km. It is usually divided further into three geomorphologically distinct reaches, including the braided, transitional, and meandering reaches (Wu et al., 2005). Heavy soil erosion in the Loess Plateau upstream has led to intensive sedimentation in the LYR. According to the observed data, the total deposition volume in the LYR reached about 5.52 billion m^3 from 1950 to 1999, of which 60% was deposited in the braided reach (Xia et al., 2009). One effect of heavy sedimentation in the LYR was characterized by an obvious shrinkage of the main channel and a sharp decrease of the flood discharging capacity, which severely influenced the management of flood control and made the phenomenon of "secondary perched river" more serious (Xia et al., 2009). Therefore, river engineers and scientists in China adopted various methods to study the morphodynamic processes in the LYR, and these methods usually comprised physical river modelling and mathematical river modelling (Zhang & Xie, 1993). With the rapid development of computers and numerical methods for nonlinear analysis during the last four decades, mathematical river models have become more popular. Two-dimensional (2D) models capable of simulating the morphodynamic processes have been developed since the end of the 1990s (Wang et al., 2008). At present, depth-averaged 2D models are more often adopted in practice when simulating the morphological changes in the LYR for their easy implementation and applications.

The application of 2D morphodynamic models to the LYR is a challenging task at the present time, although various models have been developed for and applied to this river. Lots of development efforts are still required to be investigated before these models can be applied by the managers of the LYR. In the current study, an intercomparison of three morphodynamic models is presented by considering both the difference between

the model concepts and the discrepancy in the simulated results and corresponding data measured in 2004, and some experience from this intercomparison is then gained and the most urgent model improvements for simulating the morphodynamic processes in the LYR are proposed.

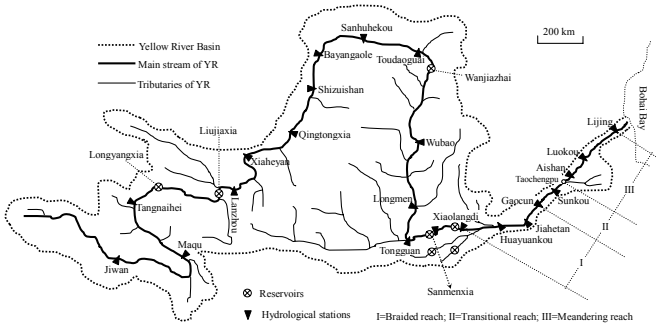

Figure 1 Sketch of the Yellow River Basin

2 COMPARISON OF MODEL CONCEPTS

2.1 *General information*

Three morphodynamic models for the LYR will be compared and they are: Delft3D (Delft Hydraulics, 2003), 2DLLCDM (Xia et al., 2004) and 2DRPM (Zhou & Lin, 2008). Delft3D is a generic commercial software package, whereas the other two were specially developed for the LYR. All the three models can be considered as consisting of three modules: a hydrodynamic module, a sediment transport module and a module for updating the morphology and bed-material composition.

Delft3D was developed by WL|Delft Hydraulics in the Netherlands. It is a model system that consists of a number of integrated modules. During this study, only the Delft2D-FS mode of Delft3D is used, which comprises a 2D flow and online-sediment module in orthogonal curvilinear coordinates. 2DLLCDM is a depth-averaged 2D model for the full channel adjustment, which consists of a submodel of 2D flow and sediment transport in orthogonal curvilinear coordinates and a submodel of riverbank erosion, which is capable of predicting the processes of flood routing and longitudinal bed deformation, and simulating the process of bank erosion. 2DRPM is also a depth-averaged 2D model for the river processes of the LYR. The model is based on an unsteady flow model in the Cartesian coordinates for fixed riverbeds by Falconer (1977) and a non-equilibrium transport equation for suspended load has been included recently (Zhou & Lin, 2008).

Both Delft2D-FS and 2DLLCDM use a curvilinear mesh, whereas 2DRPM uses a rectangular mesh. The governing equations for flow and sediment transport will be presented only in the curvilinear coordinates, since the governing equations in the Cartesian coordinates can be then considered as a special case.

2.2 *Governing equations*

The governing equations usually include the equations for hydrodynamics, the equations for sediment transport, and the algorithms of updating the morphology and bed material composition. In addition, treatments of key parameters related to the equations are also presented.

2.2.1 Hydrodynamic equations

All the above three models have in common that they all use the 2D shallow water equations (Wang et al. 2008). The depth-averaged continuity equation for flow can be written as:

$$\frac{\partial Z}{\partial t}+\frac{1}{C_\xi C_\eta}\frac{\partial}{\partial \xi}\left(hUC_\eta\right)+\frac{1}{C_\xi C_\eta}\frac{\partial}{\partial \eta}\left(hVC_\xi\right)=0 \tag{1}$$

The momentum equations for flow in the ξ and η directions are given by:

$$\begin{aligned}&\frac{\partial U}{\partial t}+\frac{U}{C_\xi}\frac{\partial U}{\partial \xi}+\frac{V}{C_\eta}\frac{\partial U}{\partial \eta}+\frac{UV}{C_\xi C_\eta}\frac{\partial C_\xi}{\partial \eta}-\frac{V^2}{C_\xi C_\eta}\frac{\partial C_\eta}{\partial \xi}\\&=-\frac{g}{C_\xi}\frac{\partial Z}{\partial \xi}-gn^2\frac{U\sqrt{U^2+V^2}}{h^{4/3}}+\frac{\nu_t}{C_\xi C_\eta}\left(\frac{\partial^2 U}{\partial \xi^2}+\frac{\partial^2 U}{\partial \eta^2}\right)\end{aligned} \tag{2}$$

$$\begin{aligned}&\frac{\partial V}{\partial t}+\frac{U}{C_\xi}\frac{\partial V}{\partial \xi}+\frac{V}{C_\eta}\frac{\partial V}{\partial \eta}+\frac{UV}{C_\xi C_\eta}\frac{\partial C_\eta}{\partial C_\xi}-\frac{V^2}{C_\xi C_\eta}\frac{\partial C_\xi}{\partial \eta}\\&=-\frac{g}{C_\eta}\frac{\partial Z}{\partial \eta}-gn^2\frac{V\sqrt{U^2+V^2}}{h^{4/3}}+\frac{\nu_t}{C_\xi C_\eta}\left(\frac{\partial^2 V}{\partial \xi^2}+\frac{\partial^2 V}{\partial \eta^2}\right)\end{aligned} \tag{3}$$

in which ξ and η = orthogonal curvilinear coordinates in the horizontal directions; Z = water level; h = water depth; U and V = velocity components in the ξ and η directions, respectively; C_ξ and C_η = *Lami* coefficients; ν_t = horizontal turbulent viscosity coefficient for flow; g = gravitational acceleration, n = Manning's roughness coefficient; and t = time.

(1) Influence of sediment on the hydrodynamics

The sediment concentrations in the LYR are extremely high, so that the density of the water-sediment mixture becomes temporally and spatially varying, which in turn influences the turbulent structure of the flow. In the mode of Delft2D-FS only the density variation is considered. Both 2DLLCDM and 2DRPM cannot directly account for the influence of concentrations on the flow governing equations. It is applicable because sediment concentrations to be simulated are relatively low, with the maximum value < 20 kg/m^3.

(2) Formulation of bed roughness coefficient

In the LYR, the Manning's roughness coefficient was found to be quite large during low discharges,

with the highest measured value > 0.045. Following the increase of a discharge, the coefficient gradually reduced and approached a minimum of 0.007 to 0.010 (Chien et al., 1959).

In Delft3D, the roughness coefficient is specified as a constant, or as a space-varying Manning's coefficient, or computed with a bed roughness predictor (van Rijn, 2007a). However, this roughness predictor has not been extensively validated in rivers such as the LYR. Therefore, only constant roughness values are used in the present study for Delft3D. Similarly, constant roughness values are used for 2DRPM. 2DLLCDM uses the formula by Zhao & Zhang (1997) to calculate the Manning's roughness coefficient, given by

$$n=\frac{h^{1/6}}{\sqrt{g}}\frac{c_n\delta_*}{h}\left\{0.49(\frac{\delta_*}{h})^{0.77}+\frac{3\pi}{8}(1-\frac{\delta_*}{h})[\sin(\frac{\delta_*}{h})^{0.2}]^5\right\}^{-1} \quad (4)$$

in which c_n = 0.375κ; and δ_* = roughness thickness. This formula is valid for the flow Froude number less than 0.80.

2.2.2 Sediment transport equations

In the LYR, the change in morphology is mainly caused by the non-equilibrium transport of suspended load, which is closely related to the determination method of source term, and the formulation of sediment transport capacity.

(1) Equation for bed load transport

In simulating sediment transport, Delft3D always includes both bed load and suspended load transport. The other two models do not include the simulation of bed load transport because in the river the suspended load is fairly dominant. According to the analysis by Long & Zhang (2002), the average ratio of bed load to total load of sediment in the LYR is only about 0.5%.

(2) Equation for suspended load transport

The advection-diffusion equation for the fractional suspended load transport used in the three models can be given as

$$\frac{\partial(hS_k)}{\partial t}+\frac{1}{C_\xi C_\eta}\left[\frac{\partial}{\partial\xi}(C_\eta UhS_k)+\frac{\partial}{\partial\eta}(C_\xi VhS_k)\right] =\frac{h}{C_\xi C_\eta}\left\{\frac{\partial}{\partial\xi}[\varepsilon_s\frac{C_\eta}{C_\xi}\frac{\partial S_k}{\partial\xi}]+\frac{\partial}{\partial\eta}[\varepsilon_s\frac{C_\xi}{C_\eta}\frac{\partial S_k}{\partial\eta}]\right\}+E_k-D_k \quad (5)$$

where ε_s = horizontal turbulent diffusivity coefficient for sediment; S_k = sediment concentration for the *k*th size fraction; and the source term is represented by the rates of bed erosion (E_k) and deposition (D_k), respectively. The three models adopt different expressions for these terms.

(3) Calculation of the source term

2DLLCDM and 2DRPM apply a similar equation for the source term of each fraction, given by:

$$D_k-E_k=\alpha_{sk}\omega_{sk}\left(S_k-S_{*k}\right) \quad (6)$$

in which S_{*k} and α_{sk} are the sediment transport capacity and coefficient of saturation recovery or adjustment for the *k*th fraction.

In 2DLLCDM α_{sk} is determined by the method proposed by Zhang et al. (2001), while in 2DRPM α_{sk} is calculated according to the method proposed by Zhou & Lin (1998). In 2DLLCDM and 2DRPM, all the fractions of suspended load are regarded as noncohesive sediments. In Delft3D, for non-cohesive fractions Eq. (6) is also used to calculate the source term, but the coefficient α_{sk} is calculated according to Galappatti (1983). For cohesive fractions, the Krone-Partheniades formulations are used to calculate the source term (Partheniades, 1965).

(4) Sediment transport capacity

Delft3D uses formulas that calculate either the total sediment transport or the bed load and suspended load separately. From the suspended load, an equilibrium sediment concentration can be derived, which is used to obtain a depth-averaged concentration in combination with an advection-diffusion equation, given by:

$$S_*=\int_a^h u(z)c(z)dz\,/\int_a^h u(z)dz \quad (7)$$

where a = reference height above the bed; $u(z)$ = velocity profile; $c(z)$ = concentration profile; and z = integration variable. In this study, the enhanced sediment formula of Van Rijn is applied (Van Rijn, 2007ab). This formula can calculate the sediment transport capacity of the total load. The enhanced formula has been developed for sediments with a grain size of 0.008 mm and coarser, for concentrations up to 150 kg/m^3 and water depths exceeding 1.0 m.

In 2DLLCDM, the sediment transport capacity formula proposed by Zhang and Zhang (1992) is used, which can be written as:

$$S_*=2.5[\frac{(0.0022+S_v)u^3}{\kappa[\gamma_s-\gamma_m)/\gamma_m]gh\omega_m}\ln(\frac{h}{6D_{50}})]^{0.62} \quad (8)$$

where S_* = sediment transport capacity in kg/m^3; γ_s and γ_m = specific densities of sediment and water, respectively; S_v = sediment concentration by volume; $u=\sqrt{U^2+V^2}$; κ = Von Karman coefficient for turbid water; ω_m = group settling velocity of non-uniform sediments; and D_{50} = median diameter of the bed material. This formula has been widely used in the computation of sediment transport in the LYR.

According to the data of Zhang & Xie (1993), Zhou & Lin (2008) obtained a simplified form of sediment transport capacity formulation as

$$S_* = k(u^3 / gh\omega_m)^m \quad (9)$$

in which $k = 0.606$, and $m = 1.636 - 0.216\mathrm{Log}(u^3 / gh\omega_m)$. Eq. (9) is used in 2DRPM.

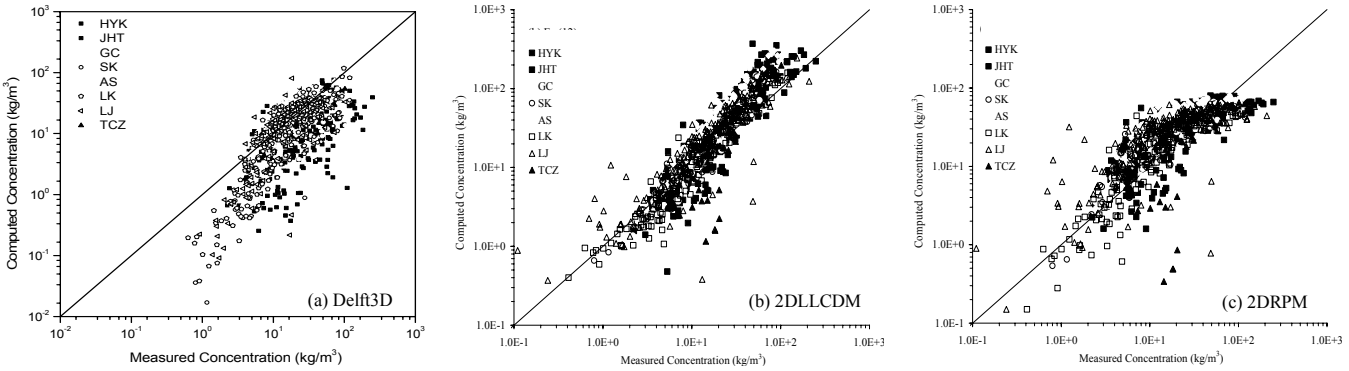

Figure 2 Comparison between the calculated and observed concentrations

Eqs. (7-9) can be used to calculate the sediment transport capacity for the total suspended load. If ΔP_{*k} is the percentage of the sediment transport capacity for the *k*th grain size, the expression of $S_{*k} = S_* \Delta P_{*k}$ can be obtained. In the above-mentioned three models, different approaches were used to determine the value of ΔP_{*k}. Figure 2 compares the results computed by the above formulas with the observed data, and it can be found that: Eq. (7) underpredicts the sediment transport capacity if the concentration is less than 10 kg/m^3 although it overestimates at high concentrations; Eq. (8) performs well because it was calibrated by the data from the Yellow River; and Eq. (9) overestimates the concentration as it ranges in 10 to 100 kg/m^3.

2.2.3 Updating the morphology

In updating the morphology in the LYR, the rate of longitudinal channel adjustment can be determined using the bed deformation equation due to the non-equilibrium transport of suspended load, while the lateral channel adjustment needs to adopt the simulation of bank erosion.

(1) Updating bed level

2DLLCDM and 2DRPM only account for the transport process of suspended load. Therefore, the change in bed level can be calculated by:

$$\rho' \frac{\partial Z_b}{\partial t} = \rho' \sum_{k=1}^{N} \left(\frac{\Delta Z_{bk}}{\Delta t} \right) = \sum_{k=1}^{N} \left(D_k - E_k \right) \quad (10)$$

in which Z_b = bed level; ρ' = dry density of bed material; ΔZ_{bk} = thickness of bed erosion or deposition for *k*th size fraction; N = total number of sediment fractions; and Δt = time step. Delft2D-FS still includes bed load transport, and therefore the change of bed level is extended with the divergence of the bed load transport.

(2) Bank erosion simulation

In the braided reach, bank erosion often occurs during the period of clear water scour, due to the water impoundment and sediment detention of the Xiaolangdi Reservoir. Analysis of observed data showed that the scour amount in the braided reach was 0.59 billion m^3, and the sediment quantity from bank erosion accounted for 30-50% (Xia et al., 2007). At present, bank erosion is not accounted for in 2DRPM. Delft3D uses a dry cell erosion factor to simulate the process of bank erosion (Roelvink et al., 2003). 2DLLCDM simulates bank erosion based on hydrodynamics and soil mechanics (Wang et al., 2008).

2.2.4 Updating the bed material composition

In 2DLLCDM, the bed material at each cell is divided into two vertical layers: the upper one is called the mixing layer and the lower one is called the memory layer. The adjustment procedure of the size distribution of surface bed material can be classified into two cases of bed scour and bed deposition, with the details being given in Wang et al. (2008). Delft3D uses a similar procedure as 2DLLCDM. However, the former usually accounts for the adjustment of bed material in the mixing layer. In 2DRPM, the memory layer is divided into 2 larger layers, and other treatments are identical to those of 2DLLCDM.

2.3 *Numerical solution methods*

In Delft3D, the model domain is usually covered by a curvilinear mesh, and the variables are arranged on a staggered grid to discretize the 2D shallow water equations in space. In this arrangement, a water level point is defined in the centre of a cell and the velocity components are located on the grid cell faces. Stelling & Leendertse (1991) extended the alternating-direction-implicit (ADI) method of Leendertse (1970) with a special approach for the advection terms. The scheme is known as a Cyclic method of ADI. The sediment transport equation is formulated in a conservative form and is solved using the Cyclic method.

2DLLCDM uses a three-step solution procedure. First, the flow governing equations are split into two sets of equations in the longitudinal and lateral directions using the method of fractional steps (Yanenko, 1971). The "time marching" ADI scheme is employed to solve the two sets of discretized equations on a staggered grid (Leendertse, 1970). Secondly, a method of fractional steps in space and a hybrid scheme are used to solve the transport equation of suspended load. Thirdly, the bed elevation at each node by the end of the time level can be obtained with the explicit scheme, and updating the bed material composition is then conducted (Wang et al., 2008).

2DRPM is based on the 2D model of DIVAST proposed by Falconer (1977). A new module of simulating the non-equilibrium transport of graded sediments is implemented, including the computation of transport capacity for fractional sediments, treating the bed deformation, updating the bed material composition and estimating the adjustment coefficient for sediment transport.

3 MODEL SET-UP

According to the flood defence law of the Chinese government, water levels in reservoirs along the Yellow River need to be lowered to a certain elevation before the flood season. A large volume of water would be released during this period. In order to optimise the use of the water, large-scale experiments of a joint operation between several associated reservoirs have been undertaken recently, and detailed hydrological data were collected along the river. In the study, the above models were set up to simulate a water and sediment regulation experiment conducted in 2004.

3.1 *Computational grid and initial bathymetry*

The study domain covered an 87 km long reach between Jiahetan and Gaocun in the LYR, with 46 observed sections, and it was divided into 472×10 curvilinear cells. The bed elevation of each cell was obtained from the observed cross-sectional geometry by interpolation. This mesh was used by Delft3D and 2DLLCDM. 2DRPM used a mesh with a regular grid spacing of 69 m, where the bed elevation of each cell was interpolated from the bathymetry of the curvilinear mesh.

3.2 *Boundary conditions*

The upstream boundary was located at Jiahetan, 220 km downstream of the Xiaolangdi Dam. The downstream boundary was located at Gaocun. Figure 3 shows the observed processes of discharge and concentration at Jiahetan, and water level at Gaocun. The study period was 600 hours, and the time step of 6 seconds was used.

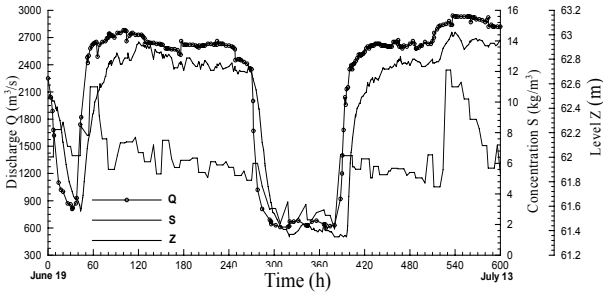

Figure 3 Boundary conditions used in the models

3.3 *Initial bed material composition*

The size distributions of bed material were available at only 8 cross-sections observed in April 2004, so the nodal gradation was obtained by interpolation. Sediment compositions for both suspended load and bed material were non-uniform, and five fractions were used to represent the mixture, with their diameters of 8, 23.50, 46.50, 93.50 and 250.0 μm. The first fraction was treated as cohesive sediment, whereas other fractions were treated as non-cohesive sediments in Delft3D. At the initial time, the mean median diameter of bed material was 0.056 mm, which was coarser than that of suspended load at Jiahetan.

4 ANALYSIS OF MODEL RESULTS

The most common calibration parameter for hydrodynamics is bed roughness, whereas the calibration parameters for morphology are numerous. In this study a different approach was followed because numerous datasets with high accuracy were not readily available for the LYR, but the calibration parameters themselves were a part of the analysis. Therefore, the model-predicted hydrodynamic and morphologic results are analysed herein for each model. The effects of different bed roughness coefficients were investigated on the predicted results. Delft3D and 2DLLCDM were required to be run for a sufficiently long time without bathymetry updating to achieve a steady state, and these results were used as the initial conditions. However, a distribution of velocity and concentration everywhere of zero, and a constant water level for the domain were used as the initial values for 2DPRM.

4.1 *Effect of bed roughness on water level*

Figure 4 compares the water levels at Jiahetan computed using various roughness coefficients with the measurements. In Delft3D (Figure4a), a roughness coefficient of 0.012 provides the best agreement between the simulated and measured

levels. 2DLLCDM can satisfactorily simulate the water levels when Eq. (4) is used. In Figure 4c, the water levels calculated by 2DRPM are in close agreement with the measurements if a constant roughness value of 0.015 is used. If a value of 0.010 is used, the water levels are greatly underestimated. In addition, the calculated levels disagree with the observed data in the early tens of hours for any roughness value due to the incorrect input of initial conditions. Therefore, the initial values influence the calculated results during the early period. It is necessary to input the appropriate initial conditions. The common way to deal with this is to adopt a spin-up period for all the models.

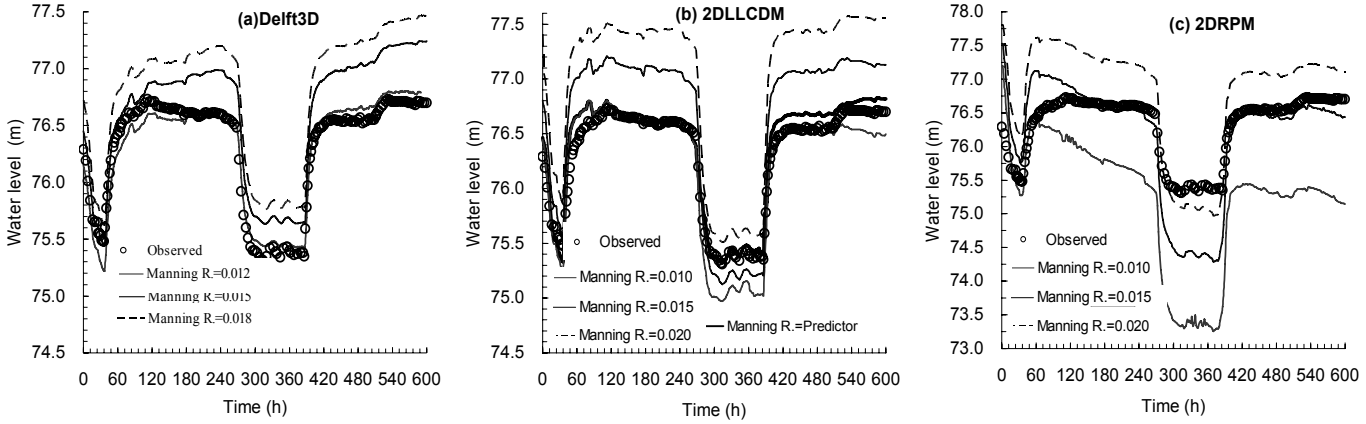

Figure 4 Comparison between the calculated levels using different roughness values and observed data

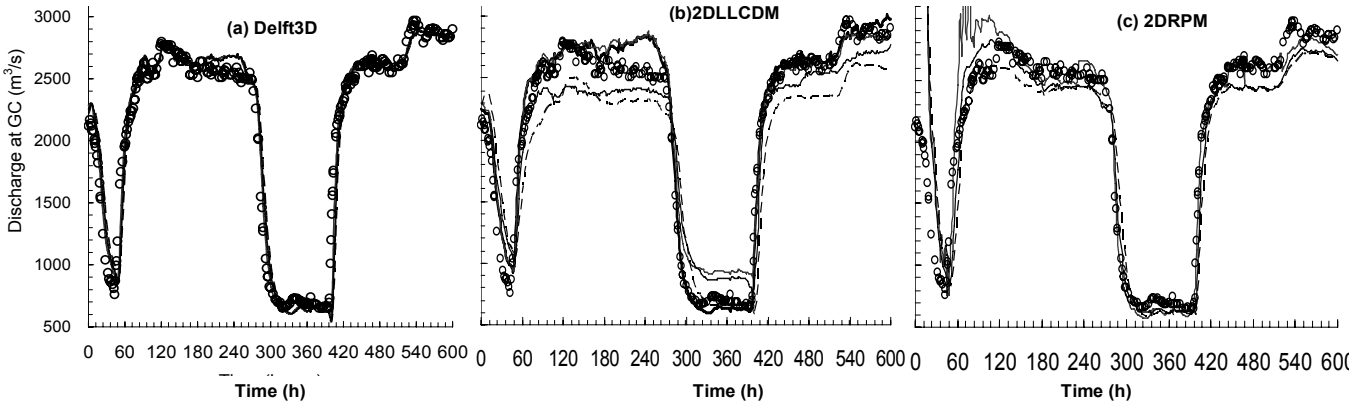

Figure 5 Comparison between the calculated discharges using different roughness values and observed data

4.2 *Effect of bed roughness on discharge*

Figure 5 compares the discharge hydrographs at Gaocun calculated by different roughness coefficients with the observed data. The effect of bed roughness on the discharges predicted by Delft3D is slight, as shown in Figure 5a. The calculated two peak discharges are in good agreement with those observed. Figure 5b indicates that different roughness coefficients have a slight influence on the predicted discharges by 2DLLCDM. Some oscillations occur in the discharges calculated by 2DRPM during the early 120 hours (Figure5c), which was caused by the input of inappropriate initial values. This comparison indicates that: (i) the roughness coefficient only has a little effect on the predicted discharges, and a lower value improves the simulated results; and (ii) in order to avoid unphysical oscillation in the calculations, a spin-up period is required for all the models.

4.3 *Effect of bed roughness on concentration*

Figure 6 compares the sediment concentrations of suspended load at Gaocun calculated using different roughness coefficients with the observed data. Temporal variation in suspended load concentration calculated by Delft3D (Figure 6a) is similar to that in the observed data, and the concentrations computed with a roughness value of 0.012 agree better with the observations. In 2DLLCDM (Figure 6b), the concentrations computed using the roughness predictor are in close agreement with the measurements during the early period, while they are underestimated during the second flood peak. The concentrations computed by 2DRPM (Figure6c) with various roughness values can not agree with the measurements. The above results indicate: (i) the concentrations predicted by Delft3D and 2DLLCDM are in close agreement with the measurements if an appropriate roughness coefficient is used; and (ii) as compared with the capability of predicting the water levels and discharges, the capability of predicting the concentrations by 2DRPM is relatively weak, which means the accuracy of the sediment transport capacity formulation needs to be improved.

4.4 *Effect of bed roughness on lateral profiles*

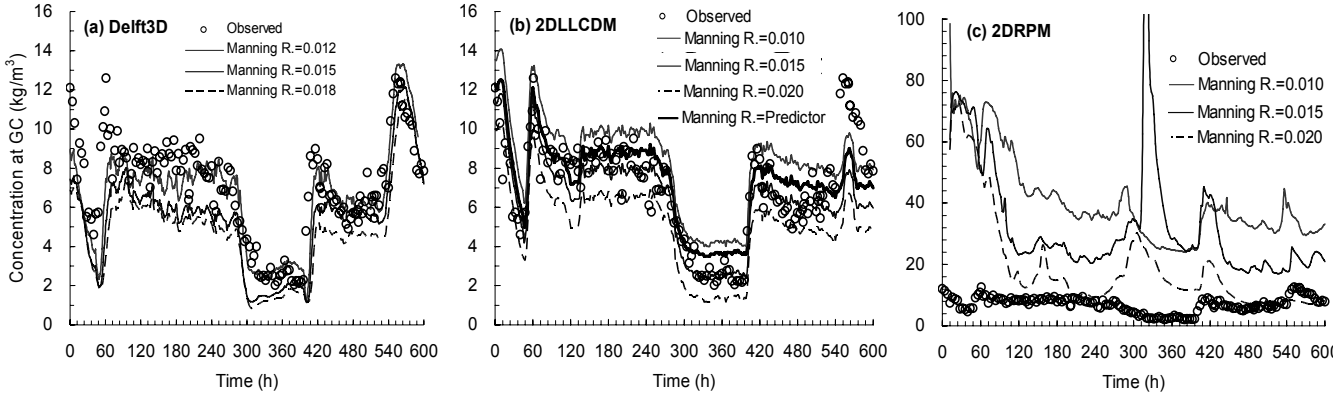

Figure 6 Comparison between the calculated concentrations using different roughness values and those observed

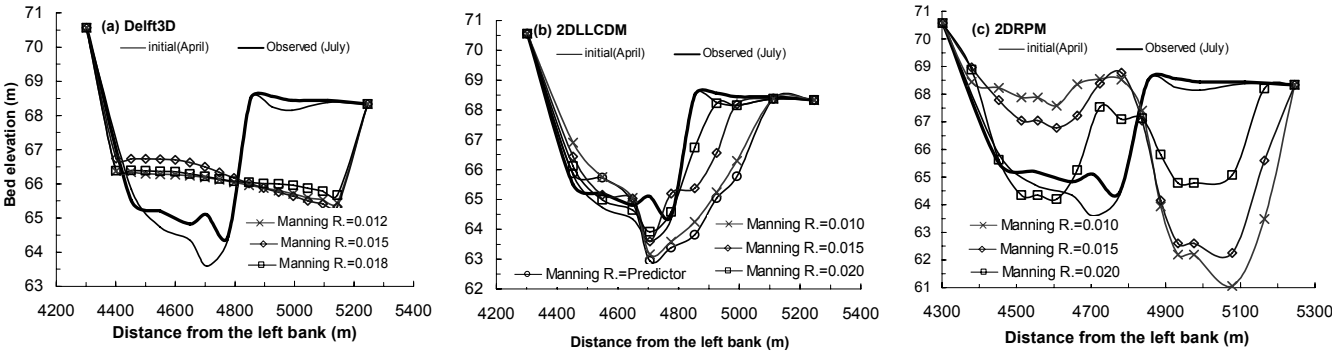

Figure 7 Comparison between the calculated profiles using different roughness values and that observed

Figure 7 compares the predicted changes in cross-sectional geometry at section of CS29 with different roughness coefficients with that observed. CS29 was located about 48 km downstream of the inlet section. In Delft3D (Figure 7a), the simulated profiles with different roughness values are characterized by about 390 m retreat of the right floodplain bank, independent of any roughness value used. However, this section did not experience any bank erosion. In 2DLLCDM (Figure 7b), different values of the bed roughness only have a slight effect on the changes of lateral profile at CS29, and all the simulated profiles with different roughness values show bank erosion although no bank erosion was observed. 2DRPM (Figure 7c) predicts great channel shifting in the profile at CS29, whereas only channel deepening was observed. In addition, different roughness values caused considerable diversity in the predicted profiles, and this phenomenon could be caused by the adoption of the formulations of sediment transport capacity and saturation recovery coefficient in 2DRPM. It can be seen from the simulations that these models cannot predict accurately the changes in cross-sectional geometry, which may be caused by the models themselves, and initial conditions input.

5 DISCUSSION

All the three models are unable to accurately predict the observed changes in cross-sectional geometry due to the complex morphology in the LYR. It should be pointed out that some discrepancy between the simulated and observed data was caused by the inaccuracy of input data, and a part of discrepancy was induced by the model limitations themselves.

5.1 *Inaccuracy of input data*

Inaccuracy of input data in these models concerns both the initial bathymetry and initial composition of bed material. The inaccuracy of initial bathymetry results from three aspects: (i) large spacing (2 km) existed between the two observed consecutive sections; (ii) the latest bathymetry was not available; and (iii) coarse mesh dimensions could not provide the accurate bathymetry. In addition, local sediment transport capacity is closely related to the local composition of bed material, the composition of bed material and its spatial variation influence the pattern of erosion or deposition. However, this spatial variation was not known with insufficient details.

5.2 *Model limitations*

Model limitations for the LYR cover lots of aspects. Based on the comparison between the simulated results and observed levels, it can be concluded that the bed roughness coefficient should be variable both in space and time. Therefore, the first improvement in the models is to develop a bed roughness predictor with relatively high accuracy. The accuracy of the sediment transport capacity formulas used in the models directly influences the morphological changes, and has an indirect effect on the flood routing and water levels along the reach. Of the three formulas of sediment transport capacity used, the accuracy of Eqs. (7) and (9) is relatively low. Therefore, the second improvement is to enhance the accuracy of the current formulas. Bank erosion plays an important role in the channel adjustment of the LYR, which is related to the riverbank soil composition and mechanical characteristics. Therefore, the third improvement is to develop a bank erosion module, which is based on near-bank hydrodynamics and soil mechanics, and can account for the temporal variations in shear strength and water content of riverbank soil.

6 CONCLUSIONS

In the present study, three morphodynamic models (Delft3D, 2DLLCDM and 2DRPM) were intercompared as they were used to simulate the morphodynamic processes in the LYR. The simulated results indicate that the predicted water levels and discharges from these three models can agree well with the observed data with an appropriately selected bed roughness coefficient. The predicted concentrations of suspended load at the downstream section from Delft3D and 2DLLCDM agree closely with the measurements, but the predicted concentrations from 2DRPM are much higher than the observed data. None of the three models is able to predict accurately the observed changes of cross-sectional profiles. Further discussion indicates that two factors causing the inaccuracy of simulated results were presented, including the inaccuracy of input data and model limitations. Three urgent improvements for these models have been identified, which are: the development of bed roughness predictor, the introduction of graded sediment transport capacity formulation, and the consideration of bank erosion module.

ACKNOWLEDGEMENTS

This work was supported by the Program for New Century Excellent Talents in University from the Chinese Ministry of Education (NCET-10-0619) and by the project investigating the effects of human activities on the ecomorphological evolution of rivers and estuaries (2008DFB90240).

REFERENCES

Chien, N., Mai, Q.W., Hong, R.J. and Bi, C.F. (1959). Roughness of the Lower Yellow River. Journal of Sediment Research, 4(1): 1-15 (in Chinese).

Delft Hydraulics (2003). User manual of Delft3D-Flow: simulation of multi-dimensional hydrodynamic flows and transport phenomena, including sediments.

Falconer, R.A. (1977). Mathematical modelling of jet-forced circulation in reservoirs and harbours (Ph.D. Thesis). University of London, London, 237 pp.

Galapatti, R. (1983). A depth-integrated model for suspended transport. Report 83-7, Communications on Hydraulics, Department of Civil Engineering, Delft University of Technology.

Leendertse, J.J. (1970). A water quality simulation model for well-mixed estuaries and costal seas (Vol. 1): Principles of computation. New York: Rand Corporation, RM-6230-RC, pp. 1-71.

Long, Y.Q. and Zhang, Y.F. (2002). Study on sediment transport in the Yellow River using a concept of the total load. Journal of Yellow River, (9): 28-30 (in Chinese).

Partheniades, E.A. (1965). Erosion and deposition of cohesive soils. ASCE Journal of the Hydraulics Division, 91(1): 105-139.

Roelvink, J.A., Van Kessel, T., Alfageme, S. and Canizares, R. (2003). Modelling of barrier island response to storms. In: Proceedings of Coastal Sediments 2003.

Stelling, G.S. and Leendertse, J.J. (1991). Approximation of convective processes by cyclic AOI methods. In: Proceeding of the 2nd ASCE Conference on Estuarine and Coastal Modelling, Tampa, New York, pp. 771-782.

Van Rijn, L.C. (2007a). Unified view of sediment transport by currents and waves I: initiation of motion, bed roughness, and bed-load transport. ASCE Journal of Hydraulic Engineering, 133(6): 649-667.

Van Rijn, L.C. (2007b). Unified view of sediment transport by currents and waves II: suspended transport. ASCE Journal of Hydraulic Engineering, 133(6): 668-689

Wang, G.Q., Xia, J.Q. and Wu, B.S. (2008). Numerical simulation of longitudinal and lateral channel deformations in the braided reach. ASCE Journal of Hydraulic Engineering, 134(8): 1064-1078

Wu, B.S., Wang, G.Q., Ma, J.M. and Zhang, R. (2005). Case study: river training and its effects on fluvial processes in the lower Yellow River, China. ASCE Journal of Hydraulic Engineering, 131(2): 85-96.

Xia, J.Q., Wang, G.Q. and Wu, B.S. (2004). Two-dimensional numerical modeling of the longitudinal and lateral channel deformations in alluvial rivers. Science in China (Ser. E), 47(Supp.I): 199-211.

Xia, J.Q., Wu, B.S. and Wang, Y.P. (2007). Processes and characteristics of recent channel adjustment in the Lower Yellow River. In: Proceedings of the 10th ISRS (Vol. V), Moscow, Russia, pp. 126-135.

Xia, J.Q., Wu, B.S., Wang, G.Q. and Wang, Y.P. (2010). Estimation of bankfull discharge in the LYR using different approaches. Geomorphology, 117, 66-77.

Yanenko, N.N. (1971). The method of fractional steps: the solution of problems of mathematical physics in several variables. Berlin: Springer-verlag.

Zhang, H.W., Huang, Y.D. and Zhao, L.J. (2001). A mathematical model for unsteady sediment transport in the LYR. International Journal of Sediment Research, 16(2): 150-158.

Zhang, H.W. and Zhang, Q. (1992). Formula for the sediment transport capacity of the Yellow River. Journal of Yellow River, (11):7-9 (in Chinese).

Zhang, R.J. and Xie, J.H. (1993). Sedimentation research in China. Beijing: China Water and Power Press.

Zhao, L.J. and Zhang, H.W. (1997). Study on the roughness characteristic of the Lower Yellow River. Journal of Yellow River, (9): 17-20 (in Chinese).

Zhou, J.J. and Lin, B.L. (2008). Modelling bed evolution processes in alluvial rivers. In: River flow 2008, Altinakar et al. (eds).

Zhou, J.J. and Lin, B.N. (1998). One-dimensional mathematical model for suspended sediment by lateral integration. ASCE Journal of Hydraulic Engineering, 124(7): 712-717.